

# Measurement of Contact Pressure Distribution between Spur Gear Teeth using Multi-point Thin-film Sensor

Akira Kurasako<sup>#1</sup>, Michiyasu Owashi<sup>#1</sup>, Yoshihiro Sakai<sup>#1</sup>, Yuji Mihara<sup>\*2</sup>, Hiroshi Ohue<sup>\*2</sup>

<sup>#</sup> Graduate school, Tokyo City University  
1-28-1 Setagaya-ku, Tokyo, 158-8557, Japan.  
g1181113@tcu.ac.jp

<sup>\*</sup> Department of Mechanical Engineering, Tokyo City University  
1-28-1 Setagaya-ku, Tokyo, 158-8557, Japan  
ymihara@tcu.ac.jp

**Abstract**—In order to investigate the durability of the sliding surface of machinery, it is important to know the force acting on such parts and to evaluate its stress distribution. Contact pressure occurring on the surface of gear teeth is an important factor in determining the bending stress on the gear teeth. However, since the contact area of each gear tooth surface is extremely small, a pressure sensor which can measure dynamic pressure cannot be attached. For this reason, the authors developed a thin-film pressure sensor to measure the contact pressure distribution on the gear flank. A thin-film sensor was designed to simultaneously measure contact pressure distribution in the teeth width direction. Improvement in durability could be achieved by the newly developed film structure method of this study. The measured results of pressure distribution in tooth trace direction were in good agreement with the calculations under a torque of 100Nm, in consideration of the shape of the tooth surface and misalignment. As torque increases over 150Nm, measured pressure distribution values gradually increased, and tended to become close to Hertzian pressure.

**Keywords**— Gear, Pressure distribution, Tribology, Sensor, Lubrication

## I. INTRODUCTION

Contact pressure occurring on the surface of gear teeth is an important factor to determine load capacity and to evaluate material strength and surface treatment. In order to know the contact pressure, calculated Hertzian pressure is the simplest way to sufficiently estimate the pressure [1], however, actual contact configuration of the gear tooth surface in a real machine differs from the theoretical configuration. This is caused by inaccurate assembly and deformation or slant of the shafts and bearing housings supporting the gear unit. The authors applied thin-film pressure sensor technology developed for measurement of pressure distribution of engine parts to contact pressure measurement of the gear teeth [2][3][4]. In this

study, a multi-point thin-film pressure sensor with a thickness of approximately 6 $\mu$ m and 5-point sensing parts was developed and deposited on the flank line to measure the axial pressure distribution between gear teeth. Moreover, the measured and calculated results were compared.

## II. GEAR TEST RIG

### A. Outline of The Test Rig

Fig.1 shows an overview of the power-circulating gear test rig. A thin-film pressure sensor(1) was deposited on the driving gear surface(2) and contact pressure distribution between driven gears(3) was measured. The test torque was applied to the flange shaft using a push rod(4) and torque input arm(5). Torque was transmitted to the test gear(1)(2) through the torque rod(6) from the gears (7) and (8). The test rotating speed was set at 3rpm with the servomotor installed to the shaft end(9) and the test torque was detected by the strain gauge(10) attached to the torque rod(6). Table 1 shows the specifications of test gear used for this experiment. The outer diameter of the spur gear was 91.4mm with a module of 3.

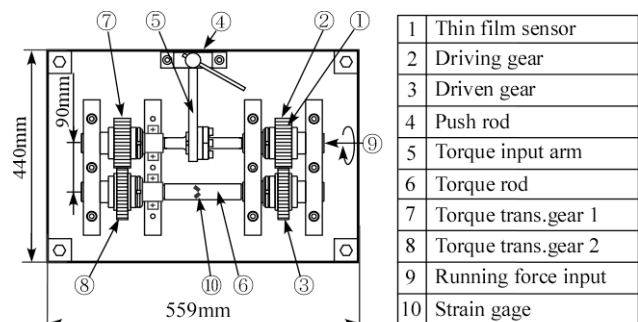


Fig.1 Gear test unit

### B. Sensor Location

Fig.2 shows the location of the 5-point sensor formed on a spur gear flank. The width of tooth flank was 30mm and each of the five sensors of P1 to P5 were formed on the tooth trace and also were axially 4mm apart with P3 set at the center of the gear flank.

Table 1 Specification of test gears

	Driving	Driven
Number of teeth $z$	28	32
Basic circle diameter $d_b$ [mm]	78.93	90.21
Pitch circle diameter $d_w$ [mm]	84.21	95.79
Tip circle diameter $d_a$ [mm]	91.41	101.79
Facewidth $b$ [mm]	30	20
Material	SCM420	
Module	3	
Young's modulus $E$ [GPa]	206	
Gear ratio $u$	1.14	
Transverse contact ratio $\epsilon_\alpha$	1.9384	
Transverse pressure angle $\alpha_t$ [deg]	20	
Working pressure angle $\alpha_w$ [deg]	20	
Transverse working pressure angle $\alpha_{wt}$ [deg]	20	

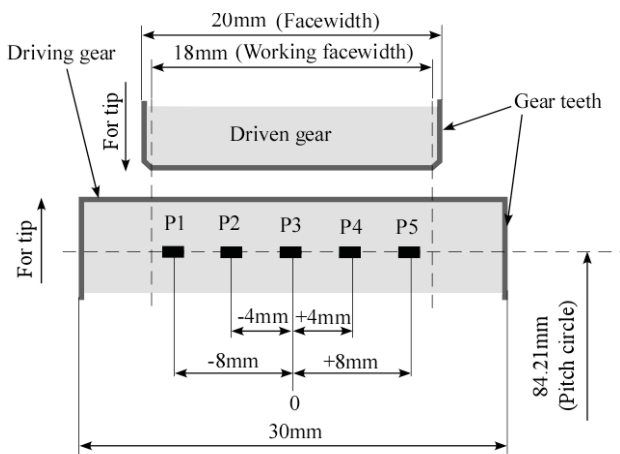


Fig.2 Location of pressure sensing point on a driving gear tooth (5-points)

### III. THIN-FILM PRESSURE SENSOR

#### A. Measurement Principle

The electrical resistance of the thin-film sensor changes under pressure. This change in resistance is converted into voltage change through a Wheatstone bridge circuit and is then amplified and recorded. Change in resistance is mostly attributable to the piezo-resistive effect, which is the change in electrical resistivity of the alloy caused by pressure.

#### B. Sensor Form

Fig.3 shows a multi-point thin-film pressure sensor deposited on a test gear. Fig.3(b) is an example of the sensor shape of the sensor. As shown in Fig.3(c), the sensor consists of a 10 $\mu$ m wide sensing part to accurately measure pressure in extremely narrow contact areas and two lead films which carry the signal out. Sensor length includes lead films was 26mm with a facewidth of 30mm. Facewidth of the driven gear was 20mm so that  $\phi$ 50 $\mu$ m lead wires attached to the end of two lead films would not interfere with the driven gear tooth flank.

#### C. Structure of Thin-Film Sensor

Fig.4 shows the film structure of the thin-film sensor. An insulation film(2) of 3.0 $\mu$ m thickness was deposited on a steel substrate(1) (gear tooth surface, SCM420). Next, a

sensing part and lead film(3) were deposited after processing by the photolithography method. A step-filler film(5) was used to compensate for the 0.2 $\mu$ m step on the surface of the protection film(4) generated by the sensing part and lead film. A 3 $\mu$ m thick protection film, deposited on the sensing part and lead film, was to prevent damage to the sensing part and lead films by the counter gear. The total film thickness of the sensor was approximately 6.2 $\mu$ m.

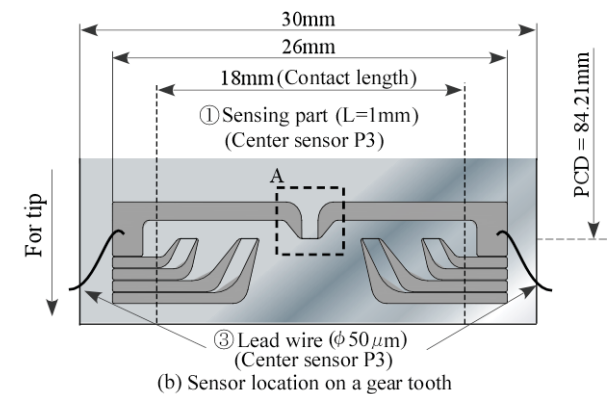
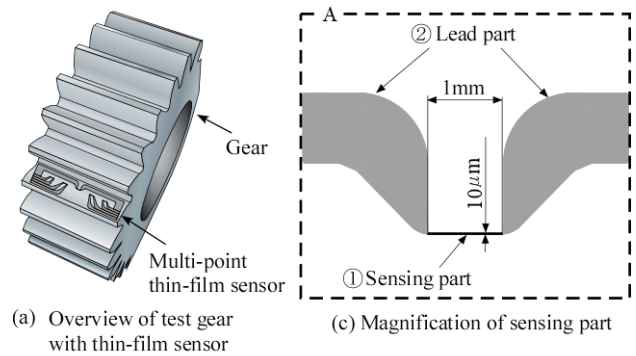


Fig.3 Overview of test gear with Multi-point thin-film pressure sensor

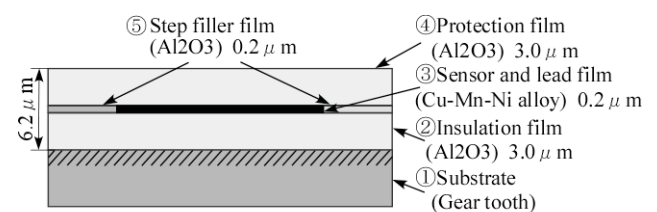


Fig.4 Structure of thin-film sensor

### IV. CALCULATED ANALYSIS OF THE CONTACT PRESSURE DISTRIBUTION

#### A. Configuration of Tooth Trace and Misalignment

Fig.5 shows the tooth trace configuration of the test gears and misalignment (inclination, deviation error) generated when the gears are meshing. As shown in Fig.5(a)(b), the driving gear has a crowning of 3 $\mu$ m in the tooth trace, and the driven gear also has 5 $\mu$ m crowning in the tooth trace. Tooth flank configuration after depositing a thin-film sensor was examined, and it was confirmed that there were no

changes in configurations of the tooth flank. Inclination and deviation error shown in Fig.5(c)(d) were measured by micro-meter and their errors were entered in the calculation.

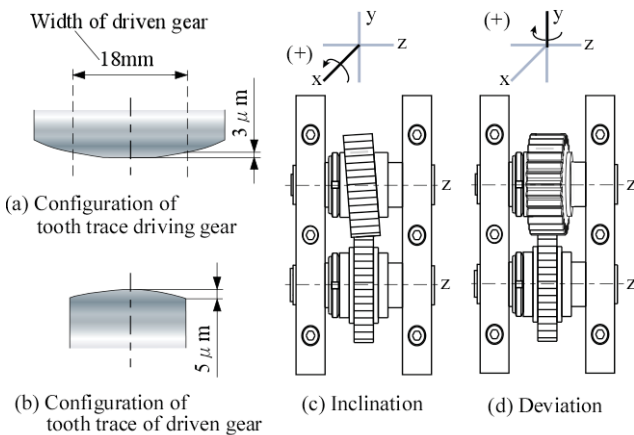


Fig.5 Tooth flank configuration and misalignment of test gears

### B. Pressure Distribution Analysis

In order to accurately compare the calculated results of contact pressure distribution with measured results, gear analysis software was used to consider both inclination and deviation error, and also the tooth flank crowning. The software prepared contact grids which function as load transfer near the contact area in addition to the conventional FEM mesh. By using this software, results could be calculated in 10 minutes. The experimental contact pressure distribution was obtained at five locations, P1-P5, as shown in Fig.2, however, contact pressure distribution by calculation was obtained from nine locations in the tooth trace in order to understand the accurate tendency of pressure distribution.

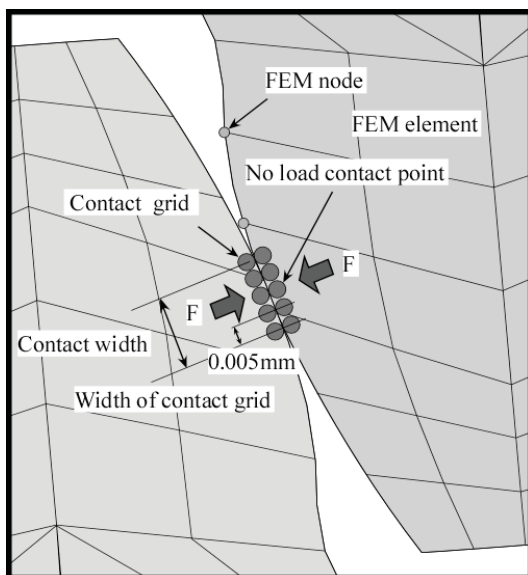


Fig.6 Calculation with the contact grid

## V. COMPARISON CONTACT PRESSURE OF CALCULATION AND MEASUREMENT

### A. Torque Condition of 30Nm and 50Nm (445MPa and 574MPa as Hertzian Pressure)

Fig.7 and Fig.8 shows the comparison results of measurement and calculation under a torque condition of 30Nm and 50Nm. A 30Nm (Hertzian pressure:445MPa), shown in Fig.7, the maximum measured pressure yielded 728MPa at P4, and the maximum calculated pressure became 777MPa at 2mm, demonstrating almost the same maximum pressure. At other locations namely P1, P2, and P5, both measurement and the calculation values resulted in 0MPa. At 50Nm torque, the maximum pressure yielded 876MPa at P4, 741MPa at P3 and the other locations, namely P1 and P5, showed 0MPa. In the calculation results at P2, P3 and P4, 495MPa, 840MPa and 756MPa, respectively were obtained. Although there was a large difference between the calculation and the experiment at P2, the same tendency at 30Nm was obtained at other measurement locations.

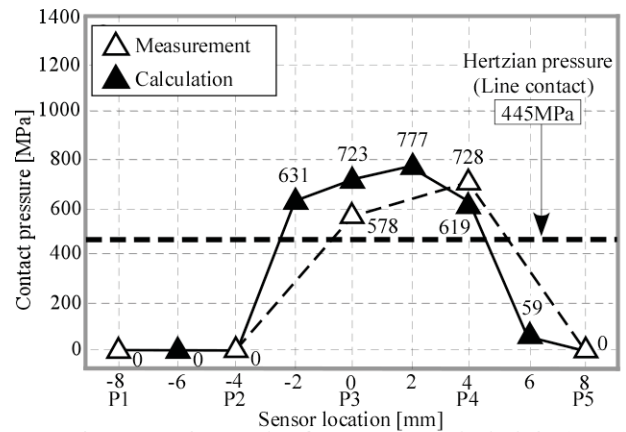


Fig.7 Comparison results of measurement and calculation(30Nm)

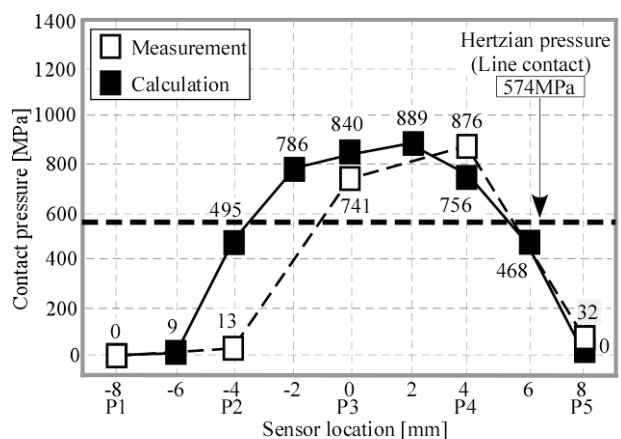


Fig.8 Comparison results of measurement and calculation(50Nm)

### B. Torque Condition of 80Nm and 100Nm (Hertzian Pressure: 727MPa and 813MPa)

Fig.9 and Fig.10 show the comparison results under a torque of 80Nm and 100Nm (Hertzian pressure: 727MPa

and 813MPa, respectively). At 80Nm, the maximum measured value yielded 1034MPa at P4, and the maximum calculated value became 1028MPa at 2mm, then, these maximum results became almost the same value. At P1, which is close to the edge of the gear flank, the measured and calculated values showed 0MPa, however, at P5, the measured result showed 414MPa. At 100Nm, the maximum measured value yielded 1086MPa at P4, and the maximum calculated value became 1110MPa at 2mm- these results became almost the same value. At P1, although the experiment and calculation values were still 0MPa, the experiment yielded 697MPa at P2, 972MPa at P3, 562MPa at P5 and the calculation 775MPa at P2 and 1059MPa at P3, and 447MPa at P5. Thus, results of the experiment and calculation at P1 through P5 agreed qualitatively and quantitatively.

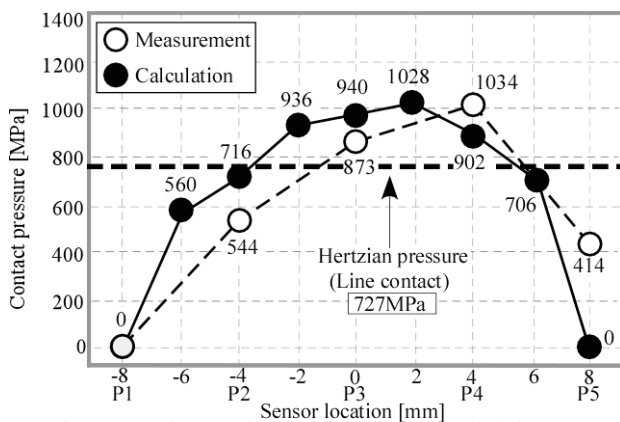


Fig.9 Comparison results of measurement and calculation(80Nm)

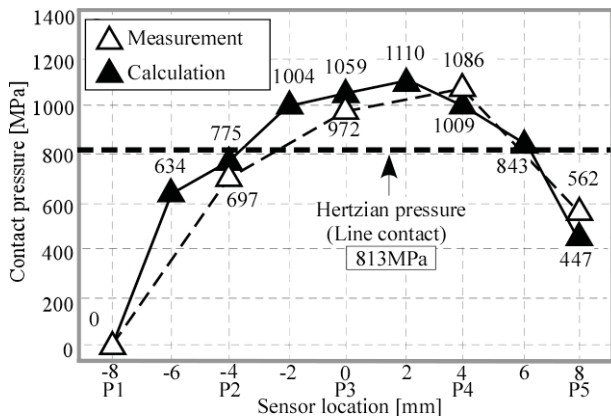


Fig.10 Comparison results of measurement and calculation(100Nm)

**C. Comparison of Calculation and Measurement Results (150 Nm and 200 Nm)(Hertzian Pressure: 996MPa and 1150MPa)**

1) Torque Condition at 150Nm: Results are shown in Fig.11. The measured values yielded 154MPa at P1, 967MPa at P2, 1103MPa at P3, 1086MPa at P4 and 925MPa at P5. In comparison with the calculation results, maximum calculation becomes 1241MPa at 2mm, and these results became almost the same value. Hence, almost same pressure in the facewidth directions began to be generated from P2 to P5. Calculation

showed almost equal pressure distribution from 1000MPa to 1200MPa in a facewidth from -6 mm to 4 mm.

2) Torque Condition at 200Nm: Measured results yielded 597MPa at P1 and P2-P5 generated 1082MPa at P2, 1140MPa at P3, 1110MPa at P4 and 1094MPa at P5. The calculated results at P1-P5 were obtained 937MPa, 1278MPa, 1342MPa, 1180MPa and 473MPa respectively. Calculation results at P1-P4 resulted higher value compared with experimental results. However, at P5, the calculation result was 621MPa lower than measured value. Also between P2 and P4, calculation increased to 1373MPa with an increase in torque, and the difference compared to the measured value was 233MPa at maximum. Measurement of P2-P5 became near Hertzian pressure of 1150MPa was obtained. From these results, measurement points gradually approach a theoretical line contact by high torque and load of occurring at the tooth flanks sharing the whole face width, and measurement values were considered to be in agreement with the calculation of Hertzian pressure.

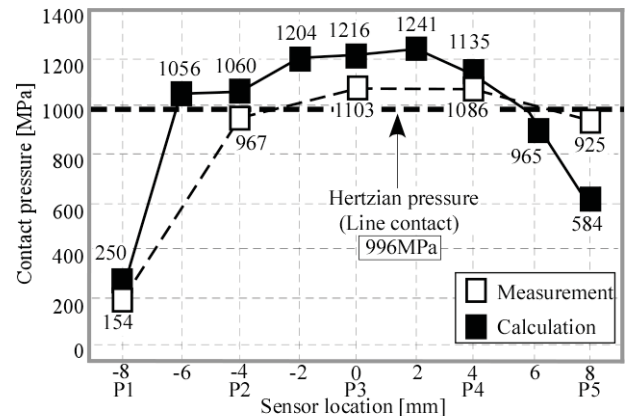


Fig.11 Comparison results of measurement and calculation(150Nm)

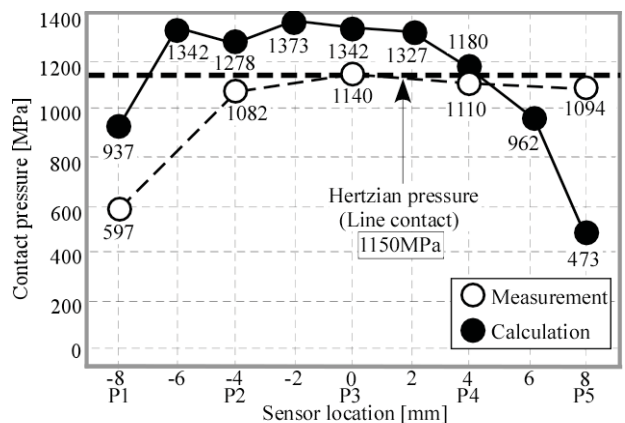


Fig.12 Comparison results of measurement and calculation(200Nm)

**VI. CONCLUSION**

(1)A multi-point thin-film pressure sensor which can measure the contact pressure of five locations of the face width direction was developed.

- (2) This sensor was directly deposited on the tooth flank by sputtering method, and the total film thickness was  $6.2\mu\text{m}$ . The sensing part had a width of  $10\mu\text{m}$  and length of  $1\text{mm}$  in order to accurately measure contact pressure in extremely narrow contact width under line contact.
- (3) The thin-film sensor consisted of an insulation film  $3.0\mu\text{m}$ , sensing and lead film  $0.2\mu\text{m}$ , step-filler film  $0.2\mu\text{m}$  and protection film  $3.0\mu\text{m}$  in thickness. The step-filler film functions to compensate for the  $0.2\mu\text{m}$  step on the surface of the protection film generated by sensing and lead film. By introducing a step-filler film, durability of the sensors increased in the experiment.
- (4) Using the multi-point thin-film pressure sensor with five-sensing parts, contact pressure distribution in the face width direction could be measured under torque conditions between  $30\text{Nm}$  to  $200\text{Nm}$  (Hertzian pressure:  $445\text{MPa}$ ,  $1150\text{MPa}$ ).
- (5) At lower torque conditions of  $30\text{Nm}$  and  $50\text{Nm}$ , contact pressure did not occur at both ends in the face width direction. This was because tooth flanks did not come into contact due to tooth crowning and gear misalignment.
- (6) At torque conditions greater than  $150\text{Nm}$ , contact pressure yielded over  $150\text{MPa}$  at each measurement location (P1-P5). Furthermore, the pressure range of  $925\text{MPa}$ - $1103\text{MPa}$  was generated at almost all measuring points, and also the pressure range of  $1082\text{MPa}$ - $1140\text{MPa}$  was generated at almost all the measuring points at  $200\text{Nm}$ . In other words, with torque increase, each pressure measuring point gradually showed near value, and pressure approached the calculated Hertzian pressure.
- (7) As a result of comparing calculations which can take crowning and misalignment into consideration, the tendency of contact pressure distribution was in good agreement. However, in conditions over  $150\text{Nm}$  torque, theoretical results acquired a gradually different tendency from a measured result.

#### REFERENCES

- [1] JGMA6102-02(2009)
- [2] Mihara, Y. et al., "Study on the Measurement of Oil-film Pressure of Engine Main Bearing by means of New Developed Thin Film Sensor under Engine Operating Conditions.", Transactions of the Society of Automotive Engineers of Japan, Vol.26, No.2(1995), pp40-45.
- [3] Mihara, Y., Someya, T., "Measurement of Oil-film Pressure in Engine Bearings Using a Thin-film Sensor", Society of Tribologists and Lubrication Engineers Paper, Vol.45(2002), pp11-20.
- [4] Mihara, Y. et al., "Measurement of piston pin-boss oil-film pressure in engine operating condition using a thin-film sensor", Transactions of the Society of Automotive Engineers of Japan, Vol. 39, No. 3 (2008), pp.125-130.